ACS OMEGA

http://pubs.acs.org/journal/acsodf

Article

Antibacterial and Anticancer Activity, Acute Toxicity, and Solubility of Co-crystals of 5-Fluorouracil and Trimethoprim

Tianping Yan, Baoyu Shu, Xuezhen Deng, Kun Qian,* Rongbin Pan, ShouLiang Qiu, Jie Yang, Qingxia Fu, and Yuexing Ma*

Cite This: *ACS Omega* 2023, 8, 21522−21530

Read Online

ACCESS | Metrics & More | Article Recommendations | Supporting Information

ABSTRACT: 5-Fluorouracil is mainly used for the treatment of tumors and has relatively high toxicity. Trimethoprim is a common broad-spectrum antibiotic agent with extremely poor water solubility. We hoped to solve these problems by synthesizing co-crystals (compound **1**) of 5-fluorouracil and trimethoprim. Solubility tests showed that the solubility of compound **1** was improved compared to that of trimethoprim. In vitro anticancer activity tests of compound **1** showed higher activity against human breast cancer cells than 5-fluorouracil. Acute toxicity showed that its toxicity was much lower than that of 5-fluorouracil. In the test of anti-*Shigella dysenteriae* activity, compound **1** showed much stronger antibacterial activity than trimethoprim.

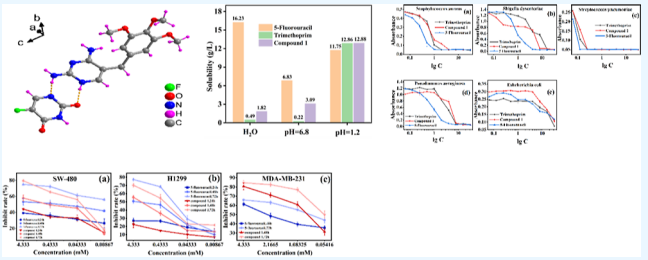

1. INTRODUCTION

Bacteria such as *Escherichia coli*, *Pseudomonas aeruginosa*, and *Staphylococcus aureus* often colonize and produce infections in cancer patients; therefore, appropriate cytostatic therapy with antimicrobial therapy can prolong the life of patients with some malignant diseases, and many antibiotic drugs are administered shortly before or after antineoplastic agents.[1,2] It is widely known that 5-fluorouracil is a commonly used antineoplastic drug, clinically used for the treatment of colon, rectal, gastric, breast, and liver cancers.[3−7] But due to the short biological half-life of 5-fluorouracil and the prominent peak and valley phenomenon of plasma drug concentration, continuous high-dose intravenous infusion is often required in clinical practice, which has caused massive damage to the patient's body.[8−10] Trimethoprim is a common broad-spectrum antibiotic agent, but it is virtually insoluble in water, poorly absorbed, and has low bioavailability, which limits its use in clinical practice.[11]

According to previous research, co-crystals are a new solid form designed using the principles of crystal engineering and supramolecular chemistry, which can significantly improve the physicochemical properties and bioavailability of drugs and are suitable for non-dissociated and weakly dissociated drugs.[12−16] Therefore, co-crystallization is an effective way to improve drug molecules' physicochemical properties; it can improve the physicochemical properties of active pharmaceutical ingredients (API), increase their bioavailability, and even extend the life of API without affecting their original biological activity.[17−19] For 5-fluorouracil, after the formation of co-crystals between 5-fluorouracil and bipyridine, nicotinamide, piperazine, hydroquinone, etc., its anticancer activity, solubility, drug selectivity, and membrane permeability were all obtained in different degrees of improvement.[20−23] For trimethoprim, the physicochemical properties improved after the formation of the co-crystals; it has been reported that the solubility and antibacterial activity of nitrofurantoin and trimethoprim are significantly enhanced after the formation of co-crystals.[24,25]

It can be seen that the drug−drug co-crystal can not only improve the physical and chemical properties of the API but also synergistically increase the efficacy of the drug and reduce side effects. Inspired by these studies, we tried to synthesize the co-crystal of 5-fluorouracil and trimethoprim. As shown in Scheme 1, 5-fluorouracil is a pyrimidine analogue with multiple N−H donors and C═O acceptors in its structure, which

Scheme 1. Chemical Structures of 5-Fluorouracil

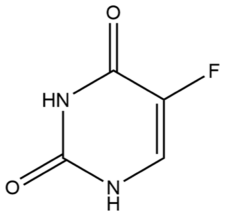

Received: January 28, 2023
Accepted: May 17, 2023
Published: June 6, 2023

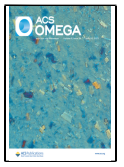

makes it prone to co-crystal formation with other compounds. Finally, we synthesized the co-crystal of 5-fluorouracil and trimethoprim successfully. The in vitro anticancer activity of compound **1** is greater against human breast cancer cells than 5-fluorouracil; acute toxicity showed that its toxicity was much lower than that of 5-fluorouracil. In the test of *Shigella dysenteriae* activity, compound **1** showed much stronger antibacterial activity than trimethoprim.

2. EXPERIMENTAL SECTION

2.1. Reagents and Solvents. 5-Fluorouracil and trimethoprim were purchased from Shanghai Bide Pharmaceutical Technology Co., Ltd and Shanghai Acme Biochemical Co., Ltd. Methanol, acetone, and hydrochloric acid were purchased from Xilong Scientific Co., Ltd and were analytically pure. Ultrapure water is self-made by an Ultrapure water machine (UPH-III-40L).

2.2. Synthesis of Compound 1. The mass ratio of 5-fluorouracil to trimethoprim is 1:2.23. The daily oral dosage of 5-fluorouracil is 150−300 mg, and the daily oral dosage of trimethoprim is 250−500 mg. According to the mass ratio, 5-fluorouracil is under the limiting dose when the therapeutic amount of trimethoprim is used as the standard. Therefore, we synthesized compound **1** by a molar ratio of 1:1.

5-Fluorouracil (1 mmol, 0.130 g) and trimethoprim (1 mmol, 0.290 g) were dissolved in 14 and 15 mL mixed solution ($V_{CH3OH}/V_{CH3COCH3}$ = 1:1), respectively. Then, they were mixed together and kept undisturbed at room temperature. Colorless crystals were obtained by the slow evaporation of the solvent. Lots of crystals are produced after 24 h.

2.3. X-ray Structure Determination. Single-crystal X-ray diffraction was performed using a Rigaku Oxford Supernova diffractometer equipped with an Oxford Cryosystems and an Atlas S2 CCD detector and employing Cu-Kα radiation generated using a sealed X-ray tube. All data were integrated within the CrysAlisPro software suite, with a face-indexed absorption correction applied to the data of each collection. The structures were solved using SHELXT,[26] with structural refinements carried out using SHELXT-2018/3[27] within the Olex2 grapHical user interface.[28] The asymmetric unit structure diagrams of compound **1** and the packing diagrams were drawn with Diamond 3.2 software.

2.4. Thermogravimetry and Differential Scanning Calorimetry. Thermogravimetric analysis of the 5-fluorouracil−trimethoprim co-crystal was carried out by a thermogravimetric/differential thermal comprehensive thermal analyzer. After drying and grinding the co-crystal, an appropriate amount of the test sample was taken into the crucible, and another empty crucible was taken as the blank control. Then, the instrument was preheated for 30 min, the heating rate was set as 10 K min^{-1}; the temperature range was set as 298−573 K, and the test was started in the N_2 atmosphere.

A differential scanning calorimeter was used to analyze the thermal behavior of the 5-fluorouracil−trimethoprim drug−drug co-crystal. After drying and grinding the co-crystal, an appropriate amount (4 mg) was accurately weighed and put into the crucible. Another empty crucible was used as the blank control. Then, the instrument was preheated for 30 min, and the test was conducted in the N_2 atmosphere with a heating rate of 10 K min^{-1} and a temperature range of 298−573 K.

2.5. Fourier Transform Infrared Tests. The Fourier transform infrared (FTIR) spectrometer (PerkinElmer Spectrum 2, USA) was turned on and preheated for 30 min. A background scan was first performed to obtain a calibration baseline for the data in the range of 4000−400 cm^{-1}. The crystals were dried and ground into a coarse and uniform powder. Then, the powder was placed on the instrument for testing in the range of 4000−400 cm^{-1}, and the IR spectra of the samples were obtained after calibration with the baseline. The obtained data were plotted and analyzed using Origin 2021.

2.6. Powder X-ray Diffraction. The X-ray powder diffractometer's X-ray source was Cu-Kα radiation (Dandong Tongda Science & Technology Co., Ltd) with a characteristic wavelength of 1.5406 Å. The instrument was preheated for 5−10 min, the voltage was 40 kV, the current was 30 mA, the angular increment was 0.02°, the test temperature was 298 K, and the test range was 5−50°; we acquired the data every 0.5 s. The crystals were ground into a coarse and uniform powder. The powder was laid flat in the powder X-ray diffraction (PXRD) quartz glass sample stage and then the quartz glass sample stage was put into the instrument for testing. The data were further processed with JADE software (Rigaku). Simulated PXRD patterns were calculated using Mercury 3.2 (Cambridge Crystallographic Data Center, UK) with a starting angle of 5°, a final angle of 50°, and a step size of 0.02°.

2.7. Hygroscopicity Test. Desiccators were prepared at 298 K and a relative humidity of 90 ± 5% with saturated potassium nitrate solution. First, the dry weighing bottle was put into the desiccator for one day before the test was conducted, then the bottle was weighted, and mass m_1 was obtained. After that, the API and co-crystals were laid in the weighing bottles with about 3 mm thickness, respectively; the bottle was weighted, and mass m_2 was obtained. Then, the bottle was placed into the desiccator for 14 days at 298 K and a relative humidity of 90 ± 5%. The weighing bottle needs to be weighed each day during the 14 days, and mass m_3 was obtained. The hygroscopicity test needs to be conducted three times of parallel tests for clarity.

$$\text{Weight gain percentage} = (m_3 - m_2)/(m_2 - m_1) \times 100\%$$

2.8. Determination of Equilibrium Solubility and Intrinsic Dissolution Rates. *2.8.1. HPLC Analysis Methods.* High-performance liquid chromatography (HPLC) analysis was conducted on an Agilent 1260 system with UV detection wavelengths of 265 nm (for 5-FU) and 271 nm (for TMP) using a C18 column (Inertsil ODS-3, 4.0 μm × 4.6 mm × 100 mm column, GL Agilent., United States of America). The column temperature was 303 K, and the injection volume was 10 μL. The mobile phase consisted of a mixture of methanol and water. The gradient elution was used with the flow rate of 1 mL/min, which was described as: 0−5 min, 10% (V/V) methanol; 5−15 min, from 10 to 90% (V/V) methanol; 15−17 min, 90% (V/V) methanol; 17−20 min, from 90 to 10% (V/V) methanol; 20−25 min, 10% (V/V) methanol.

2.8.2. Determination of Equilibrium Solubility. The equilibrium solubility of 5-fluorouracil, trimethoprim, and compound **1** in dilute hydrochloric acid solution (pH = 1.2), phosphate buffer (pH = 6.8), and pure water was determined by shaking the flask at room temperature. First, saturated solutions of 5-fluorouracil, trimethoprim, and compound **1** were prepared in the three dissolution media, respectively. Then, the saturated solution was filtered through a 0.22 μm microporous membrane, and the resulting filtrate was diluted

https://doi.org/10.1021/acsomega.3c00580
ACS Omega 2023, 8, 21522−21530

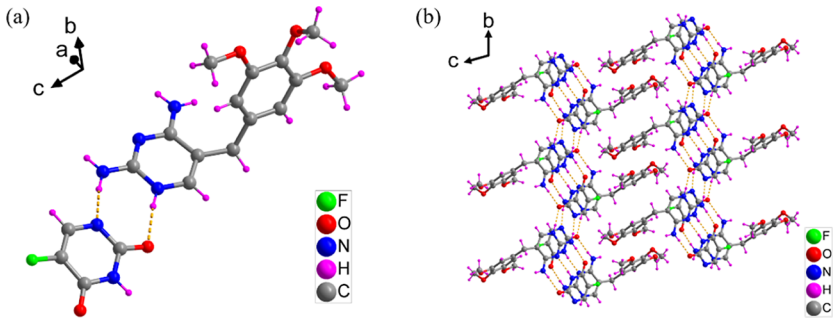

Figure 1. Asymmetric unit diagram of the co-crystal (a); packing diagram of the co-crystal (b).

to a suitable multiple with the corresponding dissolution medium; the concentration was determined with the diluted solution by the HPLC method.

2.8.3. Determination of Intrinsic Dissolution Rate. The dissolution rate was determined according to the dissolution determination method (the second method of the four general rules of the Chinese Pharmacopoeia 2020 edition for the determination of dissolution and release).[29] 250 mg of drug powder was pressed into a round tablet using a tablet press and wrapped the round tablet with solid paraffin wax, leaving only one side to contact with the dissolution medium. The tablets were immersed in 900 mL of dissolution medium (pure water) at 310 K and rotated at 100 rpm. At specific time intervals (5, 10, 15, 20, 30, 45, and 60 min), 10 mL of dissolved solution was removed and immediately filtered through a 0.22 μm microporous membrane, and the concentration was determined by using HPLC.

2.9. Antibacterial Activity Testing Analyses. The values of minimum inhibitory concentration (MIC) and minimum bactericidal concentration (MBC) of drugs in the test strain were determined by the micro broth twofold dilution method.[30,31] The trimethoprim group and compound **1** group (drug + bacterial solution + medium) were set up. Each group was set up with ten different drug concentrations (32, 16, 8, 4, 2, 1, 0.5, 0.25, 0.125, and 0.0625 μg/mL). Meanwhile, the medium control group and the bacterial solution control group (bacterial solution + medium) were set up. The animals were incubated at 310 K for 24 h, and the OD value was measured at 600 nm by a microplate reader to determine the MIC value. Incubation was continued for 48 h, and the OD value was used to determine the MBC value.

2.10. Anticancer Activity in In Vitro Assays. *2.10.1. Cell Culture.* The SW480, MDA-MB-231, and H1299 cell lines were obtained from the Integrated Chinese and Western Medicine Oncology Research Center, Jiangxi University of Chinese Medicine. All cell lines were cultured in Dulbecco's modified Eagle's medium supplemented with 10% fetal bovine serum (Sigma-Aldrich), 1% penicillin, and 1% streptomycin at 37 °C in a 5% CO_2 atmosphere. Cell growth was observed by an inverted microscope, and further experiments were performed when the cells were in the logarithmic phase (growth was 85−95% at the bottom of the flask).[32]

2.10.2. MTT Assay. The anticancer activity of compound **1** was evaluated by methyl thiazolyl tetrazolium (MTT) colorimetry with 5-fluorouracil as the positive control group in human colon cancer cells (SW480), breast cancer cells (MDA-MB-231), and lung cancer cells (H1299).[32] The cell concentration in the culture medium was adjusted to 3×10^5 cells/mL and then inoculated into 96-well plates with 200 μL per well; after 24 h of cell culture, cells were treated with different concentrations of compound **1** solution for 24, 48, and 72 h, respectively. Subsequently, methyl thiazolyl tetrazolium (MTT; 5 mg/mL, 20 μL) was added to each well and further incubated at 37 °C for 4 h. After that, the medium was discarded, and DMSO solvent (200 μL/well) was added to solubilize the formazan crystals.[33] The absorbance at the wavelength of 490 nm was measured with a multifunctional enzyme labeler, INFINITE 200 PRO, after shaking for 10 min. The mean absorbance of blank wells was used to adjust the absorbance of each experimental well.

2.11. Oral Acute Toxicity Test. *2.11.1. Preparation of Drug Doses.* Compound **1** suspension was prepared and dispersed in 0.5% sodium carboxymethylcellulose. The concentration of compound **1** corresponded to the administered dose of 3000 mg/kg-BW. The drug was provisionally prepared within 1 h prior to administration.

2.11.2. Animals and Environment. Adult Kunming mice (body weight range: 18−25 g) were purchased from the Laboratory Animal Science and Technology Center of Jiangxi University of Chinese Medicine (license no.: SCXK(Gan) 2018-0004). All mice were housed at a constant temperature of 21−25 °C and a relative humidity of 40−60% with a 12 h light/dark cycle. The mice were kept for seven days before the experiment to make them adapt to the environment. All animals were treated appropriately and used in a scientifically valid and ethical manner.

2.11.3. Pre-experiments. Trimethoprim was reported with an oral LD_{50} > 5300 mg/kg in mice, which belonged to the essentially nontoxic group, and 5-fluorouracil has an oral LD_{50} = 220 mg/kg in mice, which belonged to the toxic group.[34] Therefore, we performed pre-experiments to explore the approximate dosage range of compound **1**. We set up three dose groups of 1000, 2000, and 3000 mg/kg-BW, with six mice in each group, half of each sex. The mice were observed for 7 consecutive days after administration; no mice in the experimental groups died. Therefore, we presume that the LD_{50} of compound **1** is greater than 3000 mg/kg-BW.

2.11.4. Formal Experiment. Based on pre-experiments, we observed no acute toxicity in mice given 3000 mg/kg-BW orally. It is generally accepted that no acute toxicity or death was seen at 3000 mg/kg, and it is not necessary to increase the dose for further experiments. In addition, high-dose reactions may mask the reactions observed at lower doses, and in general, only little additional information is available for chemicals at doses above 3000 mg/kg.[35] Therefore, we chose a concentration of 3000 mg/kg-BW as the standard and used the maximum dose method to conduct acute toxicity experiments. 40 mice were selected and randomly divided into four groups

https://doi.org/10.1021/acsomega.3c00580
ACS Omega 2023, 8, 21522−21530

(blank control group, 5-fluorouracil group, trimethoprim group, and compound **1** group), with 10 mice in each group, half of each sex. The mice were fasted for 12 h before administration, administered intragastrically (0.2 mL/10 g) three times within 24 h at 4 h intervals, and fasted but not water fasted for 12 h after the last administration. The mice were observed for 14 consecutive days, and their appearance, behavior, diet, secretion, and excretion were recorded daily; their body weight was recorded on the first, fourth, seventh, and fourteenth days, respectively. After 14 days of observation, all mice were executed and dissected to observe the lesions of each organ.

3. RESULTS AND DISCUSSION

3.1. X-ray Crystal Structure. The key crystallographic parameters of compound **1** are summarized in Table S1. Compound **1** is crystallized in the triclinic system $P\bar{1}$ space group at 293(2) K with cell parameters of a = 8.5967(4) Å, b = 8.6181(4) Å, c = 13.5856(8) Å, α = 105.719(5)°, β = 90.057(4)°, γ = 93.164(4)°, and V = 967.27(9) Å^3, Z = 2. As shown in Figure 1a, the asymmetric unit of compound **1** contains one $[C_4H_2FN_2O_2]^-$ anion and one $[C_{14}H_{19}N_4O_3]^+$ cation because 5-fluorouracil misses a proton hydrogen and transfers to the nitrogen atom of the pyrimidine ring of trimethoprim. Among them, the $[C_4H_2FN_2O_2]^-$ anion with the $[C_{14}H_{19}N_4O_3]^+$ cation has two hydrogen bonds between N−H···N and N−H···O; the hydrogen bond distances are 1.974 and 1.930 Å, respectively. The packing diagram for compound **1** is drawn in Figure 1b. 5-Fluorouracil and trimethoprim are arranged to infinity by hydrogen bonding, the molecules are neatly arranged in an ordered state, and the molecular layers are parallel to each other.

3.2. Infrared Absorption Spectroscopy Analysis. The IR spectra can provide information about the molecule stretching vibration of ingredients, adjuvants, and co-crystals; thus, we compared the infrared spectrum of 5-fluorouracil, trimethoprim, and compound **1**, and the results are shown in Figure 2. Combining Figure 2 with references, we can know that in 5-fluorouracil, 1661 and 3136 cm^{-1} were attributed to the stretching vibration peaks of C═O and N−H.[36] In trimethoprim, 3471 and 3319 cm^{-1} were attributed to −NH$_2$ stretching vibration peaks, 1130 cm^{-1} was attributed to the C−O stretching vibration peaks, 1596 cm^{-1} was attributed to the stretching vibration peaks of C═C in the benzene ring, and 799 cm^{-1} was attributed to the out of plane bending vibration of the pyrimidine ring. In compound **1**, 1684 and 3148 cm^{-1} were attributed to the stretching vibration peaks of C═O and N−H, 1131 cm^{-1} was attributed to the C−O stretching vibration peaks, and 786 cm^{-1} was attributed to the out of plane bending vibration of the pyrimidine ring.[37,38]

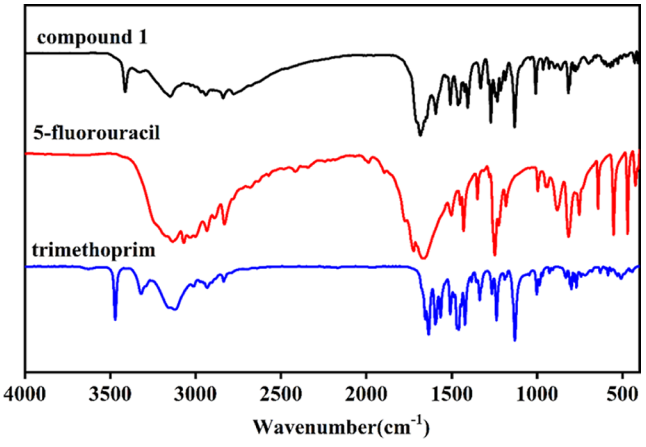

Figure 2. IR spectrum curves of trimethoprim, 5-fluorouracil, and compound **1**.

Through comparison of the infrared spectrum between 5-fluorouracil, trimethoprim, and compound **1**, we can know that after forming co-crystals, the stretching vibration peaks of C═O shifted from 1661 to 1684 cm^{-1}, the stretching vibration peaks of N−H shifted from 3136 to 3148 cm^{-1}, the out of plane bending vibration of pyrimidine ring shifted from 799 to 786 cm^{-1}, and the stretching vibration peaks of C−O shifted from 1130 to 1131 cm^{-1}. According to the comparison, the stretching vibration peaks of compound **1** shifted significantly compared to the API; from the shift, we can reasonably guess the existence of hydrogen bonds in compound **1**.

3.3. TG and DSC Analyses. We validated the thermodynamic stability of compound **1** by TG and DSC assays. The results are shown in Figure 3. The TG curve shows that the co-crystal exhibited significant weight loss at 481 K, and the co-crystal began to decompose without weight loss before the decomposition temperature decreases. From the TG curve, we can also know that the melting point of compound **1** is 482−486 K. As shown in the DSC curve, the co-crystal has no peak in heat absorption before decomposition, while the peak in heat absorption during decomposition occurs at 484 K.

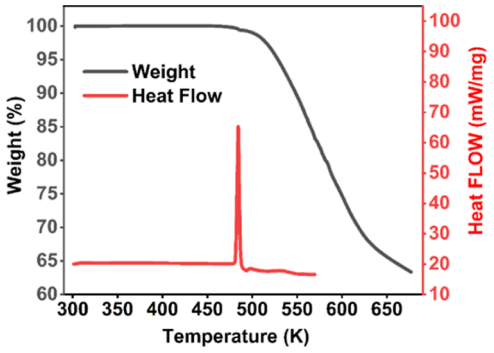

Figure 3. TG−DTA and DSC diagrams of compound **1**.

3.4. Powder X-ray Diffraction Analysis. Powder X-ray diffraction analysis (PXRD) is a method that can be used to verify the formation of a new co-crystal; we conducted powder diffraction on 5-fluorouracil, trimethoprim, and compound **1** and obtained related plots. As shown in Figure 4a, on comparing the experimented tests with stimulated tests, the position and intensity of peaks in compound **1** are consistent; therefore, compound **1** can be identified as a pure phase. According to Figure 4b, the position of the main diffraction peak in 5-fluorouracil is 22.48°, which is in accordance with the references.[39] The diffraction peaks in trimethoprim appear at 11.94, 15.24, 17.50, 18.66, 22.36, 23.82, 26.00, and 30.84°, which is also consistent with the references 37. 40, From the powder diffraction plot of compound **1**, we can know that there are no peaks in the same position as 5-fluorouracil and trimethoprim, and new highly intensive peaks appear at 6.76, 10.34, 14.12, and 24.6°, all of which confirmed that compound 1 is a new co-crystal.

https://doi.org/10.1021/acsomega.3c00580
ACS Omega 2023, 8, 21522−21530

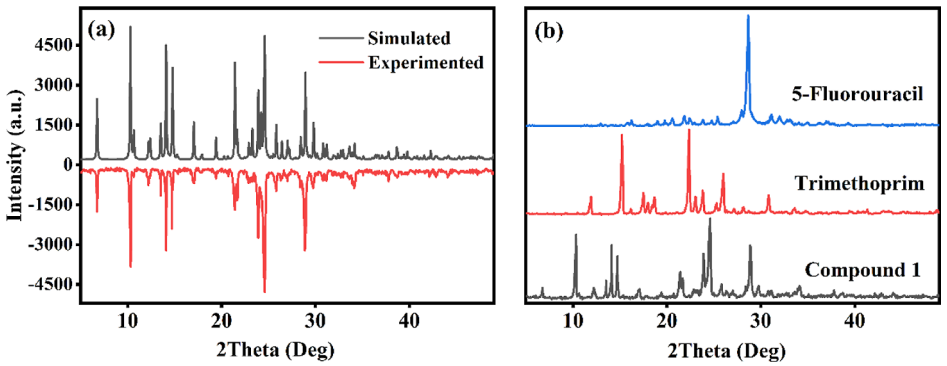

Figure 4. Comparative PXRD patterns of compound **1** and simulate compound **1** (a); PXRD patterns of 5-fluorouracil, trimethoprim, and compound **1** (b).

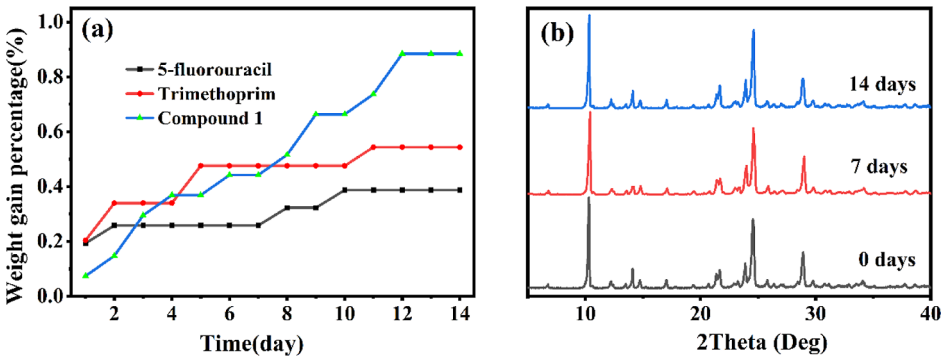

Figure 5. Hygroscopicity test results of 5-fluorouracil, trimethoprim, and compound **1** (a); powder diffractograms of compound **1** (b).

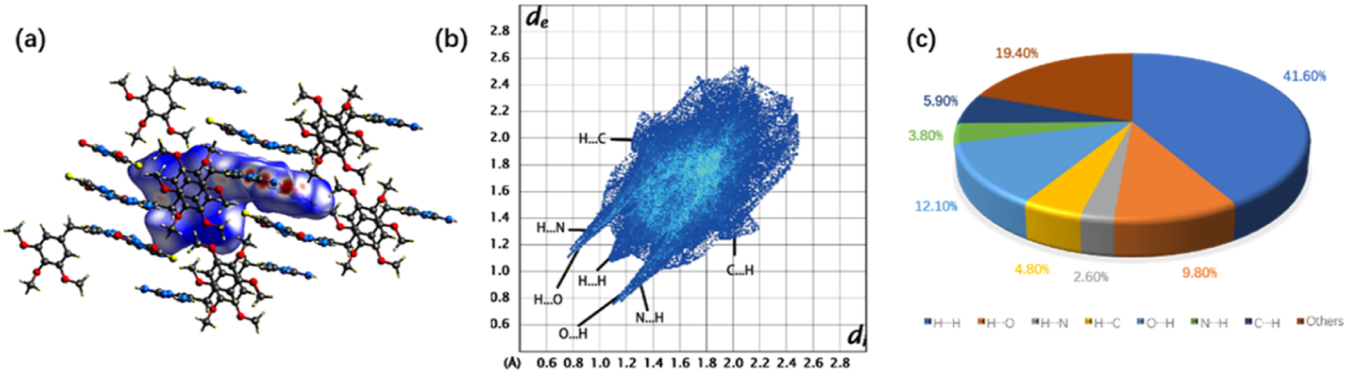

Figure 6. Hirshfeld surface analyses of compound **1**: Hirshfeld surface of compound **1** (a); 2D fingerprint plot of compound **1** (b), and pie chart of compound **1** (c).

3.5. Hygroscopicity Test Analyses. As shown in Figure 5a, the percentage weight gain of 5-fluorouracil was 0.19% on the first day, which then stabilized at 0.26% for the next six days and finally stabilized at 0.39% without further increase. The percentage weight gain of trimethoprim was 0.20% on the first day, then stabilized at 0.48% for the next nine days, and finally stabilized at 0.54% without further increase. The percentage weight gain of compound **1** was only 0.07% on the first day but gradually increased from day 2 to day 11 and finally stabilized at 0.88% without further increase. According to the Chinese Pharmacopoeia, the definition of hygroscopicity is according to weight gain (deliquescence, absorbing enough water to form a liquid; very hygroscopic ≥ 15%; hygroscopic ≥ 2%; slightly hygroscopic ≥ 0.2%; none or almost no moisture < 0.2%).[29] Therefore, 5-fluorouracil, trimethoprim, and compound **1** are all slightly hygroscopic.

3.6. Hirshfeld Surface and Fingerprint Plot Analyses. To better understand the mutual effect among the molecules, we used the crystal explorer program to draw the 3D Hirshfeld surface maps and 2D fingerprint plots by importing the crystallographic information file into the program.[41] The 3D Hirshfeld surface maps were generated with d_{norm} using a red−white−blue color scheme, and the 2D fingerprint plots were generated with the d_e and d_i distances. We drew the 3D Hirshfeld surface maps and 2D fingerprint plots of compound **1**.

As shown in Figure 6a, the red regions represent shorter contacts, the white regions were issued for contacts around the r^{vdW} separation, and the blue regions represent longer contacts in the Hirshfeld surface of compound **1**. To understand the contribution of each element's interactions to the Hirshfeld surface more intuitively, we made a pie chart. From Figure 6b,

https://doi.org/10.1021/acsomega.3c00580
ACS Omega 2023, 8, 21522−21530

we can know that the contribution of H···H interactions to the Hirshfeld surface occupies the most important place with 41.6%. To better visualize the contribution of the interaction of each element to the Hirshfeld surface, we made pie charts. As shown in Figure 6c, the H···H and O···H/H···O interactions occupied the largest part in all interactions in compound **1**, while the other interactions played a small proportion.

3.7. Solubility Analysis. The solubility of a drug affects the in vitro activity of the target molecule. To examine the solubility of the drugs, we tested the solubility of 5-fluorouracil, trimethoprim, and compound **1** in pure water, phosphate buffer (pH = 6.8), and dilute hydrochloric acid solution (pH = 1.2), respectively, and the results are shown in Figure 7. From

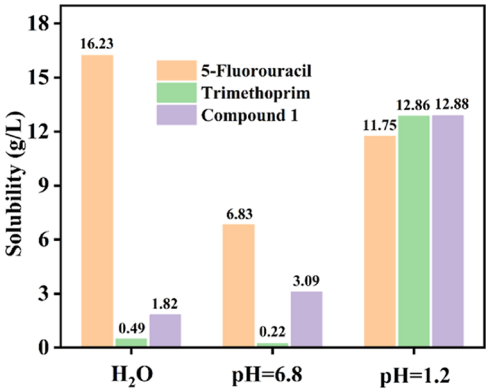

Figure 7. Solubility test results of 5-fluorouracil, trimethoprim, and compound **1** at different pHs.

the results, it can be seen that trimethoprim had the worst solubility with a value of 0.4884 g/L in water. The solubility of compound **1** was 3.7 times that of trimethoprim, indicating the improved water solubility of trimethoprim after forming a co-crystal. In phosphate buffer, 5-fluorouracil, trimethoprim, and compound **1** had solubilities of 6.8346, 0.2234, and 3.0933 g/L, respectively. From the value of the solubilities, it can be seen that compound **1** also has a higher solubility than trimethoprim. In dilute hydrochloric acid buffer, the solubilities of trimethoprim and compound **1** were 12.8551 and 12.8832 g/L, respectively, and the solubility of 5-fluorouracil was 11.7472 g/L. Obviously, the solubility of compound **1** was the largest in the hydrochloric acid buffer, which was 1.002 and 1.097 times higher than that of trimethoprim and 5-fluorouracil. The solubility of compound **1** was greater than that of trimethoprim both in pure water and in hydrochloric acid buffer, indicating that the water solubility of trimethoprim could be improved by co-crystallization; trimethoprim belongs to Biopharmacological Classification System Class II drugs, which have poor solubility, and improving its water solubility could increase the dissolution of the drug, thus improving its bioavailability in vivo.

3.8. Dissolution Rate Analysis. The dissolution rate usually determines the drug absorption rate in the body. If the dissolution rate of a drug is too slow, it will have a bad influence on the degree of absorption of the drug. But if the dissolution rate of a drug is too fast, its safety index will be low, which may bring about adverse reactions and increase the risk of drug use. In order to examine the dissolution degree of drugs, we tested the dissolution rate of 5-fluorouracil, trimethoprim, and compound **1** in water, and the results are shown in Figure 8. The figure showed that the dissolution rate

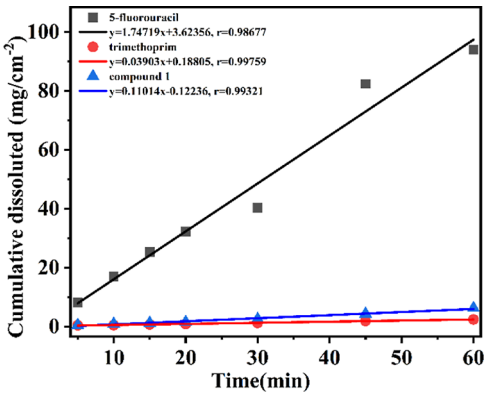

Figure 8. Intrinsic dissolution trends of 5-fluorouracil, trimethoprim, and compound **1** in water. $n = 3$, $x \pm s$.

of 5-fluorouracil was the fastest; compound **1** was the second fastest, and trimethoprim was the slowest, with IDR values of 1.747, 0.039, and 0.110 mg cm^{-2} min^{-1}, respectively. It can be seen that the dissolution rate of compound **1** was 2.82 times higher than that of trimethoprim, and the dissolution rate of trimethoprim in water was improved; the results were consistent with the solubility results. The dissolution rate of compound **1** was much lower than that of 5-fluorouracil, which decreased by 93.70%; the rapid dissolution of 5-fluorouracil improved after forming co-crystals, which provided a theoretical basis for attenuating the liver toxicity caused by the rapid dissolution of 5-fluorouracil.

3.9. Bacterial Inhibition Analyses. To investigate the antibacterial activity of compound **1**, we determined the antibacterial activity of five common bacteria (*E. coli*, *Streptococcus pneumoniae*, *S. aureus*, *S. dysenteriae*, and *P. aeruginosa*) by using the microbubble double dilution method and the Oxford cup method. Table S1 shows the data obtained by the microtiter double dilution method; we obtained the MIC and the MBC of 5-fluorouracil, trimethoprim, and compound **1**. According to Figure 9, for *E. coli*, *S. pneumoniae*, and *P. aeruginosa*, the antibacterial activity of trimethoprim and compound **1** did not show a significant difference. While for *S. aureus*, the antibacterial activity of trimethoprim was greater than that of compound **1**. But for *S. dysenteriae*, the antibacterial activity of compound **1** was higher than that of trimethoprim. It is needed to point out particularly that for these five bacteria, the antibacterial activity of 5-fluorouracil was the greatest.

3.10. Analysis of the In Vitro Anticancer Activity Assay. According to the results of anticancer activity tests, compound **1** and 5-fluorouracil all have a significant inhibition effect on human rectal cancer cells, lung cancer cells, and breast cancer cells. The inhibition was dose-dependent; the higher the concentration of the drug, the higher the rate of inhibition of cancer cells. Besides, the longer the drug treats the cancer cells, the better the inhibition effect. As shown in Figure 10c, under the same concentration and treatment time, compound **1** has a higher inhibition rate than 5-fluorouracil. We can conclude that compound **1** can significantly inhibit the proliferation and growth of breast cancer cells, which explains why compound 1 deserves further research to explore its therapeutic effect on breast cancer.

3.11. Experimental Evaluation of Acute Toxicity. The toxicity of compound **1** was analyzed according to the acute toxicity limit test and compared with the moderately toxic drug

https://doi.org/10.1021/acsomega.3c00580
ACS Omega 2023, 8, 21522−21530

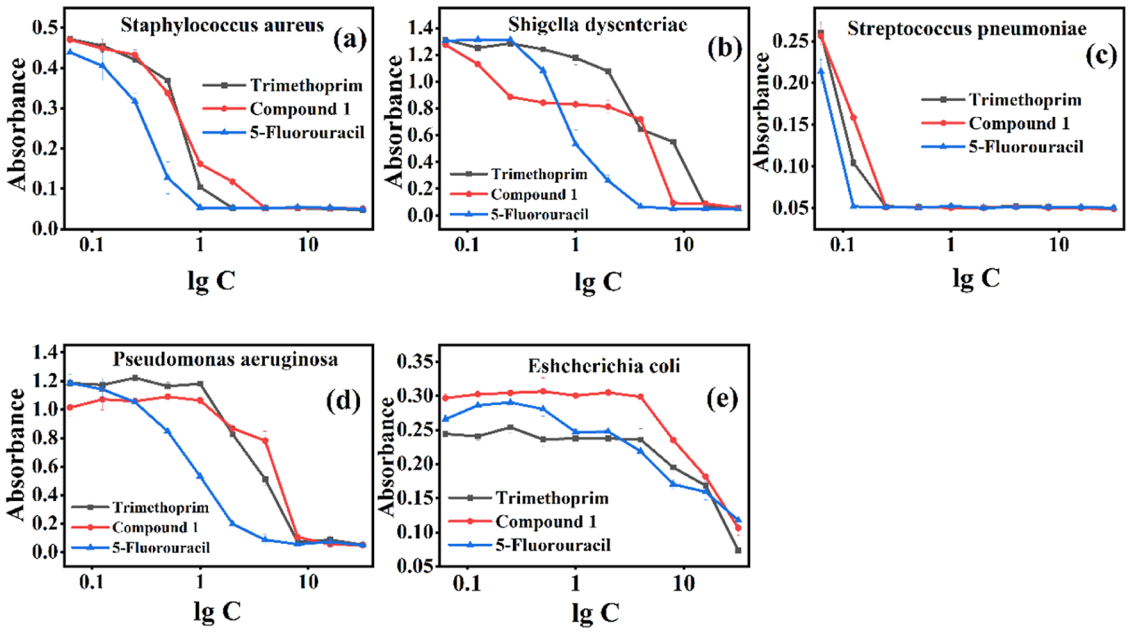

Figure 9. Antibacterial activity test results: (a) antibacterial activity test results of 5-fluorouracil, trimethoprim, and compound **1** against *S. aureus*; (b) antibacterial activity test results of 5-fluorouracil, trimethoprim, and compound **1** against *S. dysenteriae*; (c) antibacterial activity test results of 5-fluorouracil, trimethoprim, and compound **1** against *S. pneumoniae*; (d) antibacterial activity test results of 5-fluorouracil, trimethoprim, and compound **1** against *P. aeruginosa*; and (e) antibacterial activity test results of 5-fluorouracil, trimethoprim, and compound **1** against *E. coli*.

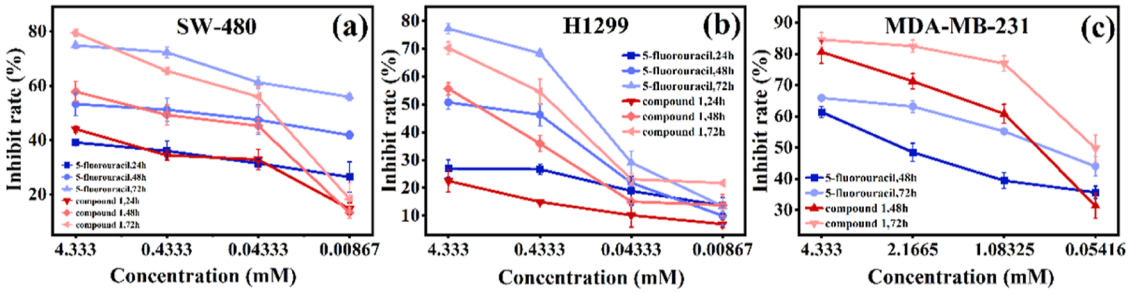

Figure 10. In vitro anti-cancer activity test results: (a) anti-cancer activity test results of 5-fluorouracil, trimethoprim, and compound **1** against SW-480; (b) anti-cancer activity test results of 5-fluorouracil, trimethoprim, and compound **1** against H1299; and (c) anti-cancer activity test results of 5-fluorouracil, trimethoprim, and compound **1** against MDA-MB-231.

5-fluorouracil to verify whether the toxicity was reduced. As shown in Table S2, one day after administration, the weight of mice in all groups decreased because of the emergency response after fasting and gavage. Seven days after administration, all mice in the 5-fluorouracil group died. After the autopsy, the liver was found to be darker black-red with more severe lesions due to the moderate toxicity of 5-fluorouracil. The mice in the blank control group and trimethoprim group all grew normally after 14 days of feeding; the internal organs were observed through the autopsy, and no lesions were observed. In the compound **1** group, seven mice finally lived in good health after drug administration, and all of them were slowly gaining weight; three mice died after seven days, and no lesions were observed. From the experimental results, it can be seen that the toxicity of compound **1** is significantly lower than that of 5-fluorouracil. In addition, according to the WHO classification criteria for oral exogenous toxicants, compounds were classified as low-toxicity drugs when their LD_{50} was 501−5000 mg/kg-BW. The LD_{50} of compound **1** was in this interval, so compound **1** was a low-toxicity drug.

4. CONCLUSIONS

In this paper, 5-fluorouracil−trimethoprim co-crystals were prepared and characterized. According to tests, the solubility of compound **1** was higher than that of trimethoprim, which improved its water solubility. The antibacterial test showed that the antibacterial activity of compound **1** against *S. dysenteriae* was higher than that of trimethoprim, and the anticancer activity test in vitro showed that compound **1** had more extraordinary ability to inhibit human breast cancer cells than 5-fluorouracil. Meanwhile, the acute toxicity test showed that compound **1** is a low-toxicity drug, which can be safely used for disease treatment. All the properties of compound **1** showed that it has the potential to be exploited. It is worth noting that most drug conjugations occur between drugs of the same type; we explored the possibility of conjugation of different types of drugs through co-crystal technology to provide a reference for future research. Due to the limitation of our knowledge, this research is only theoretical, and more data need clinical research.

https://doi.org/10.1021/acsomega.3c00580
ACS Omega 2023, 8, 21522−21530

These data can be obtained free of charge from The Cambridge Crystallographic Data Centre via www.ccdc.cam.ac.uk/data_request/cif

■ ASSOCIATED CONTENT

Supporting Information

The Supporting Information is available free of charge at https://pubs.acs.org/doi/10.1021/acsomega.3c00580.

CCDC crystallographic data (2224445) (CIF)

MIC and MBC measurements on different microbial strains; changes in the body weight of mice in acute toxicity test; summary of crystallographic data for the co-crystal; and selected bond lengths and angles of the co-crystal at 293 K (PDF)

■ AUTHOR INFORMATION

Corresponding Authors

Kun Qian − *College of Pharmacy, Jiangxi University of Chinese Medicine, Nanchang 330006, P. R. China;* orcid.org/0009-0009-4652-8488; Email: qiankun@jxutcm.edu.cn

Yuexing Ma − *Science and Technology College of Jiangxi University of Traditional Chinese Medicine, Nanchang 330004, P. R. China*; Email: yuexing@qq.com

Authors

Tianping Yan − *College of Pharmacy, Jiangxi University of Chinese Medicine, Nanchang 330006, P. R. China*

Baoyu Shu − *College of Pharmacy, Jiangxi University of Chinese Medicine, Nanchang 330006, P. R. China*

Xuezhen Deng − *College of Pharmacy, Jiangxi University of Chinese Medicine, Nanchang 330006, P. R. China*

Rongbin Pan − *Integrated Chinese and Western Medicine Oncology Research Centre, Jiangxi University of Chinese Medicine, Nanchang 330006, P. R. China*

ShouLiang Qiu − *College of Pharmacy, Jiangxi University of Chinese Medicine, Nanchang 330006, P. R. China*

Jie Yang − *College of Pharmacy, Jiangxi University of Chinese Medicine, Nanchang 330006, P. R. China*

Qingxia Fu − *College of Pharmacy, Jiangxi University of Chinese Medicine, Nanchang 330006, P. R. China*

Complete contact information is available at: https://pubs.acs.org/10.1021/acsomega.3c00580

Notes

The authors declare no competing financial interest.

■ ACKNOWLEDGMENTS

This work was supported by the National Natural Science Foundation of China (grant 22165014); the Inherited and Innovative Group of Processing Technique of Traditional Chinese Medicine (grant no. CXTD22003); the Jiangxi Provincial Traditional Chinese Medicine Administration Project (grants 2021A328 and 2022A36); the Science and Technology Plan Project of Jiangxi Provincial Health and Health Commission (grant 02131039); the Jiangxi University of Traditional Chinese Medicine Doctoral Start-up Fund (grant 2020BSZR015); the Jiangxi Province 2022 Postgraduate Innovation Special Fund Project (YC2022-s856); and the Jiangxi Province 2022 Postgraduate Innovation Special Fund Project (JZYC22S60).

■ REFERENCES

(1) Nyhlen, A.; Ljungberg, B.; Nilsson-Ehle, I.; Odenholt, I. Postantibiotic Effect of Meropenem and Ciprofloxacin in the Presence of 5-Fluorouracil. *Chemotherapy* **2002**, *48*, 182−188.

(2) Castelli, M.; Barbieri, M. L.; Bertolini, A.; Bossa, R.; Galatulas, I. Bactericidal and Antineoplastic Effect of Combination of Norfloxacin and Adriamycin. *Chemotherapy* **1987**, *33*, 355−360.

(3) Cao, J. J.; Huang, J.; Gui, S. Y.; Chu, X. Q. Preparation, Synergism, and Biocompatibility of in Situ Liquid Crystals Loaded with Sinomenine and 5-Fluorouracil for Treatment of Liver Cancer. *Int. J. Nanomed.* **2021**, *16*, 3725−3739.

(4) Goel, G.; Ramanan, K.; Kaltenmeier, C.; Zhang, L.; Freeman, G. J.; Normolle, D. P.; Tang, D. L.; Lotze, M. T. Effect of 5-Fluorouracil on Membranous PD-L1 Expression in Colon Cancer Cells. *J. Clin. Oncol.* **2016**, *34*, S-592.

(5) Na, D.; Chae, J.; Cho, S. Y.; Kang, W.; Lee, A.; Min, S.; Kang, J.; Kim, M. J.; Choi, J.; Lee, W.; et al. Predictive Biomarkers for 5-Fluorouracil and Oxaliplatin-based Chemotherapy in Gastric Cancers via Profiling of Patient-derived Xenografts. *Nat. Commun.* **2021**, *12*, 4840−4914.

(6) Regazzoni, S.; Pesce, G.; Marini, G.; Cavalli, F.; Goldhirsch, A. Low-dose Continuous Intravenous Infusion of 5-Fluorouracil for Metastatic Breast Cancer. *Ann. Oncol.* **1996**, *7*, 807−813.

(7) Wu, C. S. Y.; Williams, T. M.; Wei, L.; Umar, H.; Mikhail, S.; Ciombor, K. K.; Noonan, A. M.; Roychowdhury, S.; El-Dika, S. S.; Krishna, S.; et al. Phase I Study of Neoadjuvant 5-Fluorouracil (5FU) Chemoradiation (CRT) and Trametinib in Patients with Locally Advanced Rectal Cancers (LARC). *J. Clin. Oncol.* **2017**, *35*, 685.

(8) Dai, X. L.; Wu, C.; Li, J. H.; Liu, L. C.; He, X.; Lu, T. B.; Chen, J. M. Modulating the Solubility and Pharmacokinetic Properties of 5-Fluorouracil via Co-crystallization. *Crystengcomm* **2020**, *22*, 3670−3682.

(9) Mattos, A. C. d.; Altmeyer, C.; Tominaga, T. T.; Khalil, N. M.; Mainardes, R. M. Polymeric Nanoparticles for Oral Delivery of 5-Fluorouracil: Formulation Optimization, Cytotoxicity Assay and Preclinical Pharmacokinetics Study. *Eur. J. Pharm. Sci.* **2016**, *84*, 83−91.

(10) Ewert de Oliveira, B.; Junqueira Amorim, O. H.; Lima, L. L.; Rezende, R. A.; Mestnik, N. C.; Bagatin, E.; Leonardi, G. R. 5-Fluorouracil, Innovative Drug Delivery Systems to Enhance Bioavailability for Topical Use. *J. Drug Delivery Sci. Technol.* **2021**, *61*, 102155.

(11) Mistri, H. N.; Jangid, A. G.; Pudage, A.; Shah, A.; Shrivastav, P. S. Simultaneous Determination of Sulfamethoxazole and Trimethoprim in Microgram Quantities from Low Plasma Volume by Liquid Chromatography-tandem Mass Spectrometry. *Microchem. J.* **2010**, *94*, 130−138.

(12) Chen, J. M.; Wu, C. B.; Lu, T. B. Application of Supramolecular Chemistry on Pharmaceutical Co-crystals. *Chem. J. Chin. Univ.* **2011**, *32*, 1996−2009.

(13) Kumar, S.; Nanda, A. Approaches to Design of Pharmaceutical Co-crystals: A Review. *Mol. Cryst. Liq. Cryst.* **2018**, *667*, 54−77.

(14) Lin, Y. L.; Yang, H.; Yang, C. Q.; Wang, J. Preparation, Characterization, and Evaluation of Dipfluzine-Benzoic Acid Co-crystals with Improved Physicochemical Properties. *Pharm. Res.* **2014**, *31*, 566−578.

(15) Swarbrick, J. *Encyclopedia of Pharmaceutical Technology*; CRC Press, 2006. 9780429132728.

(16) Thakuria, R.; Delori, A.; Jones, W.; Lipert, M. P.; Roy, L.; Rodriguez-Hornedo, N. Pharmaceutical Co-crystals and Poorly Soluble Drugs. *Int. J. Pharm.* **2013**, *453*, 101−125.

(17) Dai, X. L.; Chen, J. M.; Lu, T. B. Pharmaceutical Co-crystallization: An Effective Approach to Modulate the Physicochemical Properties of Solid-state Drugs. *Crystengcomm* **2018**, *20*, 5292−5316.

(18) Wang, L. Y.; Zhao, M. Y.; Bu, F. Z.; Niu, Y. Y.; Yu, Y. M.; Li, Y. T.; Yan, C. W.; Wu, Z. Y. Co-crystallization of Amantadine Hydrochloride with Resveratrol: The First Drug−nutraceutical Co-crystal Displaying Synergistic Antiviral Activity. *Cryst. Growth Des.* **2021**, *21*, 2763−2776.

(19) Jiang, L. L.; Huang, Y.; Zhang, Q.; He, H. Y.; Xu, Y.; Mei, X. F. Preparation and Solid-state Characterization of Dapsone Drug-Drug Co-crystals. *Cryst. Growth Des.* **2014**, *14*, 4562−4573.
(20) Suresh Kumar, S.; Athimoolam, S.; Sridhar, B. Structural, Spectral, Theoretical and Anticancer Studies on New Co-crystal of the Drug 5-Fluorouracil. *J. Mol. Struct.* **2018**, *1173*, 951−958.
(21) Muresan-Pop, M.; Chereches, G.; Borodi, G.; Fischer-Fodor, E.; Simon, S. Structural Characterization of 5-Fluorouracil & Piperazine New Solid Forms and Evaluation of Their Antitumor Activity. *J. Mol. Struct.* **2020**, *1207*, 127842.
(22) Nadzri, N. I.; Sabri, N. H.; Lee, V. S.; Abdul Halim, S. N. 5-Fluorouracil Co-crystals and Their Potential Anti-Cancer Activities Calculated by Molecular Docking Studies. *J. Chem. Crystallogr.* **2016**, *46*, 144−154.
(23) Zhang, Z. Y.; Yu, N.; Xue, C.; Gao, S.; Deng, Z. P.; Li, M.; Liu, C.; Castellot, J.; Han, S. Y. Potential Anti-Tumor Drug: Co-crystal 5-Fluorouracil-Nicotinamide. *ACS Omega* **2020**, *5*, 15777−15782.
(24) Ton, C. Q.; Egert, E. The Co-crystallization of Trimethoprim with Glutarimide Derivatives by Means of Molecular Recognition. *Acta Crystallogr., Sect. A: Found. Adv.* **2010**, *66*, S228.
(25) Maity, D. K.; Paul, R. K.; Desiraju, G. R. Drug-Drug Binary Solids of Nitrofurantoin and Trimethoprim: Crystal Engineering and Pharmaceutical Properties. *Mol. Pharmaceutics* **2020**, *17*, 4435−4442.
(26) Sheldrick, G. M. SHELXT - Integrated Space-group and Crystal-structure Determination. *Acta Crystallogr., Sect. A: Found. Adv.* **2015**, *71*, 3−8.
(27) Sheldrick, G. M. Crystal Structure Refinement with SHELXL. *Acta Crystallogr., Sect. C: Struct. Chem.* **2015**, *71*, 3−8.
(28) Dolomanov, O. V.; Bourhis, L. J.; Gildea, R. J.; Howard, J. A. K.; Puschmann, H. OLEX2: A Complete Structure Solution, Refinement and Analysis Program. *J. Appl. Crystallogr.* **2009**, *42*, 339−341.
(29) National Pharmacopoeia Commission. *Pharmacopoeia of the People's Republic of China*; China Medical Science and Technology Press, 2020, ISBN 9787521415759.
(30) Parvekar, P.; Palaskar, J.; Metgud, S.; Maria, R.; Dutta, S. The Minimum Inhibitory Concentration (MIC) and Minimum Bactericidal Concentration (MBC) of Silver Nanoparticles Against Staphylococcus Aureus. *Biomater. Invest. Dent.* **2020**, *7*, 105−109.
(31) Rodriguez-Melcon, C.; Alonso-Calleja, C.; Garcia-Fernandez, C.; Carballo, J.; Capita, R. Minimum Inhibitory Concentration (MIC) and Minimum Bactericidal Concentration (MBC) for Twelve Antimicrobials (Biocides and Antibiotics) in Eight Strains of Listeria monocytogenes. *Biology* **2021**, *11*, 46.
(32) Liu, H. B.; Zhou, B. Y.; Zhao, C.; Zhang, D. F.; Wu, Q. Y.; Li, Z. Q. Synthesis and in Vitro Anticancer Properties of a Novel Neodymium(III) Complex Containing Tungstogermanate and 5-Fluorouracil. *J. Coord. Chem.* **2018**, *71*, 2102−2108.
(33) Chen, G. S.; Luo, J. Y.; Cai, M. R.; Qin, L. Y.; Wang, Y. B.; Gao, L. L.; Huang, P. Q.; Yu, Y. C.; Ding, Y. M.; Dong, X. X.; et al. Investigation of Metal-Organic Framework-5 (MOF-5) as an Antitumor Drug Oridonin Sustained Release Carrier. *Molecules* **2019**, *24*, 3369.
(34) Zhang, G. Q.; Lu, A. G.; Zhang, L. *Drugs Application and Toxicity Data*; Henan Medical University Press, 1999. 9787810483025.
(35) Wei, W.; Wu, X. M.; Li, Y. J. *Experimental Methodology of Pharmacology*; People's Medical Publishing House, 2010. 9787117124782.
(36) Gautam, M. K.; Besan, M.; Pandit, D.; Mandal, S.; Chadha, R. Co-crystal of 5-Fluorouracil: Characterization and Evaluation of Biopharmaceutical Parameters. *AAPS PharmSciTech* **2019**, *20*, 149.
(37) Djellouli, F.; Dahmani, A.; Hassani, A. Characterization of the Polymorph Changes in Trimethoprim. *J. Therm. Anal. Calorim.* **2017**, *130*, 1585−1591.
(38) Ungurean, A.; Leopold, N.; David, L.; Chiş, V. Vibrational Spectroscopic and DFT Study of Trimethoprim. *Spectrochim. Acta, Part A* **2013**, *102*, 52−58.
(39) Jubeen, F.; Ijaz, S.; Jabeen, I.; Aftab, U.; Mehdi, W.; Altaf, A.; Alissa, S. A.; Al-Ghulikah, H. A.; Ezzine, S.; Bejaoui, I.; Iqbal, M. Anticancer Potential of Novel 5-Fluorouracil Co-crystals Against MCF7 Breast and SW480 Colon Cancer Cell Lines Along with Docking Studies. *Arabian J. Chem.* **2022**, *15*, 104299.
(40) Maddileti, D.; Swapna, B.; Nangia, A. Tetramorphs of the Antibiotic Drug Trimethoprim: Characterization and Stability. *Cryst. Growth Des.* **2015**, *15*, 1745−1756.
(41) Spackman, P. R.; Turner, M. J.; McKinnon, J. J.; Wolff, S. K.; Grimwood, D. J.; Jayatilaka, D.; Spackman, M. A. CrystalExplorer: A Program for Hirshfeld Surface Analysis, Visualization and Quantitative Analysis O Molecular Crystals. *J. Appl. Crystallogr.* **2021**, *54*, 1006−1011.

https://doi.org/10.1021/acsomega.3c00580
ACS Omega 2023, 8, 21522−21530